Eur. J. Biochem. **269**, 5921–5930 (2002) © FEBS 2002 doi:10.1046/j.1432-1033.2002.03316.x

Rodent α-chymases are elastase-like proteases

Yuichi Kunori[1], Masahiro Koizumi[1], Tsukio Masegi[1], Hidenori Kasai[1], Hiroshi Kawabata[1], Yuzo Yamazaki[2] and Akiyoshi Fukamizu[3]

[1]*TEIJIN Institute for Biomedical Research, Hino, Tokyo, Japan;* [2]*TEIJIN Material Analysis Research Laboratories, Tokyo, Japan;* [3]*Center for Tsukuba Advanced Research Alliance, University of Tsukuba, Tsukuba, Ibaraki, Japan*

Although the α-chymases of primates and dogs are known as chymotrypsin-like proteases, the enzymatic properties of rodent α-chymases (rat mast cell protease 5/rMCP-5 and mouse mast cell protease 5/mMCP-5) have not been fully understood. We report that recombinant rMCP-5 and mMCP-5 are elastase-like proteases, not chymotrypsin-like proteases. An enzyme assay using chromogenic peptidyl substrates showed that mast cell protease-5s (MCP-5s) have a clear preference for small aliphatic amino acids (e.g. alanine, isoleucine, valine) in the P1 site of substrates. We used site-directed mutagenesis and computer modeling approaches to define the determinant residue for the substrate specificity of mMCP-5, and found that the mutant possessing a Gly substitution of the Val at position 216 (V216G) lost elastase-like activity but acquired chymase activity, suggesting that the Val216 dominantly restricts the substrate specificity of mMCP-5. Structural models of mMCP-5 and the V216G mutant based on the crystal structures of serine proteases (rMCP-2, human cathepsin G, and human chymase) revealed the active site differences that can account for the marked differences in substrate specificity of the two enzymes between elastase and chymase. These findings suggest that rodent α-chymases have unique biological activity different from the chymases of other species.

Keywords: mast cell protease(s); chymase; elastase; chymotrypsin; substrate specificity; site-directed mutagenesis; homology modeling.

Chymase is a chymotrypsin-like serine protease expressed exclusively in mast cells (MCs), where the protease is stored within the secretary granules and released along with tryptase, heparin, and histamine in response to allergen challenge or other stimuli [1]. Although the physiological function of this protease is still unclear, it is probably involved in various allergic inflammatory reactions, cardiovascular diseases, and chronic inflammatory diseases [2]. For example, the proposed actions of chymase include induction of microvascular leakage [3], inflammatory cell accumulation [4], neutrophil and lymphocyte chemotaxis [5], stimulation of bronchial gland secretion [6], mast cell degranulation [7], extracellular matrix degradation [8–13], and cytokine metabolism [14–17].

Based on phylogenetic analyses of a large set of cDNA-derived sequences and comparison of the substrate preferences of a smaller set of purified enzymes, mammalian chymases have been divided into two families, the α- and β-chymase families [18,19]. Mice and rats have a number of chymase isozymes that belong to the α-chymase family (mouse mast cell protease-5/mMCP-5 and rat mast cell protease-5/rMCP-5) and the β-chymase family (mMCP-1, 2, 4, rMCP-1, 2, 4) [20,21]. Primates and dogs, on the other hand, are generally thought to have just a single α-chymase [22–24]. Across mammalian species, the primary structures of α-chymases are much more similar to each other than to those of the β-chymases. For example, the amino acid sequences for human chymase have 73% and 72% identity to those of rMCP-5 and mMCP-5, respectively, and mast cell protease-5s (MCP-5s) are 94% identical to each other.

Rodent β-chymases (mMCP-1, 4 and rMCP-1, 2) purified from tissues such as skin, tongue, and intestine have been shown to be typical chymotrypsin-like proteases [25,26], and α-chymases from primates and dogs are also chymotrypsin-like enzymes with specific activity against various natural substrates [22,27–30]. As might be expected based on the results of these studies and the high degrees of sequence homology with other α-chymases of primates and dogs, rodent α-chymases were predicted to be chymotrypisin-like proteases that have very similar substrate specificity to those of other α-chymases. However, much less has been known about the properties of rodent α-chymases.

To define the enzymatic properties, in the present study we prepared recombinant rMCP-5 and mMCP-5 expressed by a baculovirus system and demonstrated that both proteases have elastase-like activity and no chymotrypsin-like (chymase) activity.

Correspondence to Y. Kunori, Pharmaceutical Discovery Research Laboratories, TEIJIN Institute for Biomedical Research, 4-3-2 Asahigaoka, Hino, Tokyo 191–8512, Japan.
Fax: +81 42 5875512, Tel.: +81 42 5868282,
E-mail: y.kunori@teijin.co.jp, FZG01556@nifty.ne.jp

Abbreviations: α1-ACT, α1-antichymotrypsin; α1-AT, α1-antitrypsin; Ang, angiotensin; CTMCs, connective tissue mast cells; HNE, human neutrophil elastase; MALDI-TOF, matrix-assisted laser desorption/ionization time of flight; MMCs, mucosal mast cells; mMCP-5, mouse mast cell protease-5; *p*NA, *para*-nitroanilide; PPE, porcine pancreatic elastase; rMCP-5, rat mast cell protease-5; SBTI, soybean trypsin inhibitor; SLPI, secretary leukoprotease inhibitor.

(Received 27 August 2002, accepted 15 October 2002)

MATERIALS AND METHODS

Materials

Sprague–Dawley rats and C57BL/6 mice were purchased from Charles River Japan, Inc., Yokohama, Japan. Chromogenic peptidyl substrates were purchased from

Bachem AG, Hauptstrasse, Bubendorf, Switzerland. Phenylmethylsulfonyl fluoride, chymostatin, and soybean trypsin inhibitor (SBTI) were purchased from Boehringer Mannheim GmbH, Mannheim, Germany. Secretary leukoprotease inhibitor (SLPI) was purchased from Genzyme, Minneapolis, MN, USA.

Preparation of recombinant proteins

The cDNAs encoding rMCP-5 and mMCP-5 were obtained by RT-PCR from total RNA extracted from the trachea of a Sprague–Dawley rat and the heart of a C57B/6 J mouse, respectively. The first strand cDNA was synthesized by using cDNA preamplification system version 2 (Invitrogen, Corp.). The MCP-5 cDNAs were amplified with *LA Taq*™ polymerase (Takara, Ohtsu, Japan) and specific primers to which *Eco*RI and *Not*I restriction sites were added [sense: 5′-GACTGAATTCATGAATCCCATGCTCTGTGT-3′ and antisense: 5′-AGATGCGGCCGCTTAATTCTCCC TCAAGATCTTATTGATCC-3′ for rMCP-5, and sense: 5′-GACTGAATTCATGCATCTTCTTGCTCTTCAT-3′ (A) and antisense 5′-GACTGCGGCCGCTTAATTCTC CCTCAAGATCTTATTG-3′ (B) for mMCP-5]. The reactions were run on a thermal cycler with the following cycle program: 94 °C·1 min^{-1} (1 cycle), 94 °C·2 min^{-1}, 58 °C·2 min^{-1}, 72 °C·3 min^{-1} (25 cycles), and 72 °C· 7 min^{-1} (1 cycle). The cDNA fragments were inserted into transfer vector pFASTbac1 (Invitrogen Corp.) and confirmed by DNA sequencing. Recombinant baculovirus was generated with a Bac-to-Bac™ baculovirus expression system (Invitrogen Corp.) according to the protocol provided by the manufacturer.

Tn5 cells were grown in 3 L of Ex-Cell 405 medium (JRH Biosciences, Lenexa, KS, USA) to a density of 2×10^6 cells·mL^{-1} in 15 Erlenmeyer flasks (200 mL per flask) on a rotary shaker (75 rounds per min) and infected with the recombinant baculovirus at a multiplicity of infection of 1. After subsequent culture for 3 days at 28 °C, the culture medium was centrifuged (500 ***g***, 30 min, 4 °C), and the supernatant was collected as the recombinant protein source.

Recombinant MCP-5s were purified by a two-step procedure. First, the culture medium was applied to a column of heparin-cellulofine (Seikagaku Corporation, Tokyo, Japan) equilibrated with 20 mM Tris/HCl (pH 8.0) buffer containing 0.1 M KCl. After washing the column with same buffer containing 0.3 M KCl, the retained material was eluted with 0.7 M KCl. The eluate was mixed with 10 volumes of 20 mM Tris/HCl (pH 8.0) buffer containing 3 M KCl, and then applied to a column of phenyl-sepharose CL-4B (Amersham Biosciences Corp., Piscataway, NJ, USA) equilibrated with the same buffer containing 3 M KCl. The material retained in the column was eluted with 0.3 M KCl while monitoring the absorbance at 280 nm. The purified proteins were subjected to N-terminal sequence analysis and mass spectrometry analysis.

Activation of the proform into the mature enzyme was accomplished by treatment with bovine cathepsin C (Sigma, St Louis, MO, USA). Purified proenzymes (3 mg each) were incubated with 10 units of cathepsin C in 30 mL of 20 mM Na_2HPO_4/NaH_2PO_4 (pH 5.8) buffer containing 0.1 M KCl, 1 mM EDTA, 10 mM dithiothreitol, and 10% glycerol at 27 °C for 1 week. The reaction mixture was then applied to a column of heparin-cellurofine equilibrated with 20 mM Na_2HPO_4/NaH_2PO_4 (pH 5.8) buffer containing 0.1 M KCl. After washing the column with the same buffer containing 0.3 M KCl, the retained material was eluted with the same buffer containing 0.7 M KCl and 0.01% Tween 20. The processing of the propeptide was confirmed by N-terminal sequence analysis and mass spectrometry analysis. After determination of the protein concentration, fractions were used as a source of purified mature enzyme.

A site-directed mutagenesis was carried out by the method of Ho *et al.* [31]. The cDNA of the V216G mutant of mMCP-5 was generated by recombinant PCR using a mutagenic primer pair (sense: 5′-CAAGGCATTGCATC CTATGGACATCGGAATGCAAAGCCC-3′, and antisense: 5′-GGGCTTTGCATTCCGATGTCCATAGGAT GCAATGCCTTG-3′) in combination with primers A and B. Generation of recombinant baculovirus and expression, purification, activation, and characterization of the protein were carried out as in the wild-type MCP-5s. Throughout this paper, the amino acid residues of mMCP-5 are numbered according to the numbering system for the corresponding residues in bovine chymotrypsinogen A (chymotrypsinogen numbering).

Active site titration of MCP-5s

The activity of wild-type MCP-5s and the V216G mutant of mMCP-5 (500 ng) was titrated with human α1-antitrypsin (α1-AT) and human α1-antichymotrypsin (α1-ACT) (Sigma), respectively. After overnight incubation of protease and inhibitors at different inhibitor/enzyme molar ratios (0.1–2 : 1), residual activity was measured with peptidyl chromogenic substrates MeO-succinyl-Ala-Ala-Pro-Val-*p*NA (*p*NA, *para*-nitroanilide) and succinyl-Ala-His-Pro-Phe-*p*NA, respectively, as described in 'Enzyme assay'.

Mass spectrometry

Molecular mass measurements of recombinant MCP-5s were carried out with a Voyager-DE STR model matrix-assisted laser desorption/ionization time of flight (MALDI-TOF) mass spectrometer (Applied Biosystems, Lincoln Centre Drive Foster City, CA, USA). After 10 μL of the protein solutions (50–100 μg·mL^{-1}) were desalted with Zip Tip C4 (Millipore, Bedford, MA, USA), the elutes containing protein (90% acetonitrile, 0.1% trifluoroacetic acid in H_2O) were mixed with an equal volume of the matrix solution (the supernatant of a 33% acetonitrile containing 0.1% trifluoroacetic acid, saturated with sinapinic acid) and placed on the MALDI target. Ions were generated by irradiation with a pulsed nitrogen laser (wavelength 337 nm), and positive ions were accelerated at 25 kV and detected in the linear mode. The singly protonated ions of a standard mixture (Insulin, Thioredoxin, and Apomyoglobin; Applied Biosystems) were used as external standards to calibrate the mass spectrometer.

In order to determine the mass of the deglycosylated forms, purified proteins (2.5–5 μg) were incubated with 1 mU of glycopeptidase F (Takara, Ohtsu, Japan) in 100 mM Tris/HCl (pH 8.6) buffer in a final volume of 50 μL at 37 °C for 20 h, and the 10 μL of the sample was analyzed as described above.

Enzyme assays

The catalytic activity of the MCP-5s was determined by using the peptidyl *p*NA substrates in a 96-well plate. Each well contained 100 μL of reaction mixture composed of 100 mM Tris/HCl, pH 8.5, 3 M NaCl, 0.01% Tween 20, and 1 mM substrate. The reaction was initiated with each MCP-5 (1 μM), and changes in absorbance at 405 nm were continuously monitored for 5 min at 25 °C with a V_{max} kinetic microplate reader (Molecular Devices Corp., Sunnyvale, CA, USA).

Kinetic analyses were carried out at seven or eight substrate concentrations (final 0.025–5 mM) by using *p*NA substrates that were hydrolyzed at 1 mM by MCP-5s. The kinetic constants K_m and V_{max} were calculated from the initial rates of hydrolysis by Lineweaver–Burke plots using linear regression. The correlation coefficients were > 0.99 in all experiments. The k_{cat} values were calculated from $V_{max}/[E] = k_{cat}$, where [E] is the concentration of enzyme. Human chymase (2 nM; Calbiochem Novachem, San Diego, CA, USA) was also examined as a control.

Inhibitor profiles

The inhibitor profiles of MCP-5s were examined at constant substrate (1 mM, MeO-succinyl-Ala-Ala-Pro-Val-*p*NA for MCP-5s, succinyl-Ala-His-Pro-Phe-*p*NA for V216G mutant) and enzyme concentrations (1 μM) in the presence of different concentrations of inhibitors in 100 mM Tris/HCl, pH 8.5, 3 M NaCl, and 0.01% Tween 20. Each enzyme was preincubated with the inhibitor on ice for 10 min, and the reaction was initiated with the substrate solution. Residual activity was monitored, and percent inhibition was calculated from the uninhibited rate. Human chymase (2 nM) and human neutrophil elastase (HNE) (2 nM; Athens Research and Technology, Inc., Athens, GA, USA) were also examined as controls with the respective substrates (MeO-succinyl-Ala-Ala-Pro-Val-*p*NA for HNE, and succinyl-Ala-His-Pro-Phe-*p*NA for human chymase).

Elastolytic activity assay

The elastolytic activitiy of MCP-5 was determined with an EnzChek® Elastase assay kit (Molecular probes, Inc., Eugene, OR, USA) according to the protocol provided by the manufacturer, with slight modification. Briefly, the DQ™-Elastin was dissolved to 50 $\mu g \cdot mL^{-1}$ in assay buffer [100 mM Tris/HCl (pH 8.5) containing 0.15 M NaCl], and 100 μL of the aliquot was mixed with 100 μL of activated MCP-5 (5, 10, 20 $\mu g \cdot mL^{-1}$ in assay buffer). Samples were incubated at 37 °C, and the fluorescence intensity at an excitation wavelength of 485 nm and an emission wavelength of 535 nm was measured at each time point (0, 60, 150 min) with a Wallac 1420 ARVO-sx Multi-label counter (Perkin Elmer Life sciences, Wellesley, MA, USA). Elastolytic activity is expressed as amounts of fluorescence. HNE was also examined at concentration of 100, 200, 500, and 1000 $ng \cdot mL^{-1}$ as a control.

Homology model building

The sequence of mMCP-5 was obtained from the SWISSPROT [32] database. A homology search of the Protein Data Bank was carried out by using the FASTA and BLAST programs, and human chymase, rat mast cell protease (rMCP)-2, and human cathepsin G were found to have sequence homology with mMCP-5 (74.8, 54.7 and 44.4%, respectively).

The homology model of mMCP-5 was constructed by using human chymase (1KLT), rMCP-2 (3RP2), and human cathepsin G (1CGH) crystal structures as templates. These three sequences and that of mMCP-5 were used for multiple alignment analysis in an Insight-II2000/homology module. All steps of homology model building and refinement were carried out by MODELLER [33]. The input files were generated by the INSIGHTII2000/homology module based on the alignment file. The modeling procedures of MODELLER were implemented using standard parameters and a database of proteins with known 3D structures. Ten models were created with medium level energy minimization and no loop optimization options. Although human chymase and human cathepsin G were determined as complex structures with inhibitors, the tertiary structures of mMCP-5 have no inhibitors. In order to validate the output structure of homology modeling and select the best model, profiles-3D and visual inspection of constructed models in INSIGHTII2000 were carried out, and the energy and PDF (probability density function) values were checked.

The V216G mutant structure was built by amino acid substitutions in INSIGHTII2000. The configurations of the residues were adopted from the rotation library of the INSIGHTII2000/homology module. No energy minimization was carried out in regard to the mutant structure.

Other methods

DNA sequence analysis was carried out with an Applied Biosystems 310 genetic analyzer (Applied Biosystems, Lincoln Centre Drive Foster City, CA, USA). SDS/PAGE analysis was performed using 10–20% polyacrylamide gel (Daiichi Pure Chemicals, Tokyo, Japan) under reducing conditions according to Laemmli [34]. Proteins were visualized by silver staining. Protein concentrations were determined with a micro-BCA protein assay kit (Pierce, Rockford, IL, USA) with bovine serum albumin as the standard. N-Terminal amino acid sequence analysis was carried out with a Hewlett Packard G1005A protein sequencing system using Edman degradation.

RESULTS

Preparation of recombinant proteins

Recombinant rat MCP-5 (rMCP-5) and mouse MCP-5 (mMCP-5) were expressed and secreted into the culture medium of Tn5 cells infected with each recombinant baculovirus. SDS/PAGE analysis following purification by chromatography on a phenyl-sepharose CL-4B column showed that each recombinant protein was essentially pure and according to its molecular weight consisted of a major 31 kDa protein and minor 30 kDa protein (Fig. 1, lanes 1 and 3). N-Terminal amino acid sequencing of the respective purified proteins yielded the consensus sequence NH_2-Gly-Glu-Ile-Ile-Gly-Gly-Thr-Glu-Pro, corresponding to the N-terminus of the pro-enzyme form of MCP-5 (proMCP-5) [21,36]. However, MALDI-TOF analysis of each protein

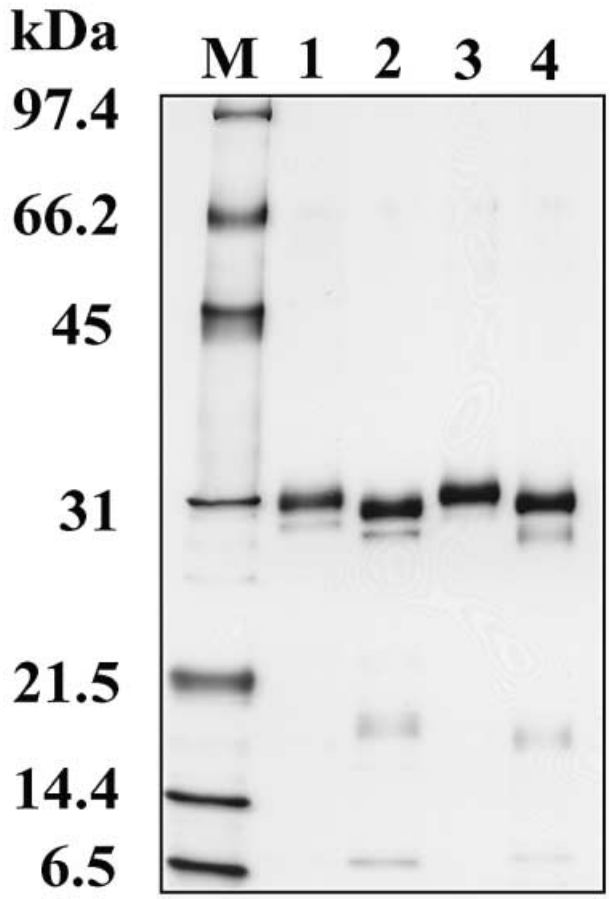

Fig. 1. SDS/PAGE analysis of purified recombinant MCP-5s. Recombinant rMCP-5 and mMCP-5 were expressed by a baculovirus system and purified as described in Experimental procedures. Purified MCP-5s were applied to 10–20% SDS/PAGE gels and visualized by silver staining. M, molecular mass standards; lane 1, pro-rMCP-5; lane 2, mature-rMCP-5; lane 3, pro-mMCP-5; lane 4, mature-mMCP-5. All samples were analyzed under reducing conditions.

yielded heterogeneous molecular masses (five or six heterogeneous signals in the range of *m*/*z* 25 500–27 000). As both enzymes carried one putative N-glycosylation site at Asn79 [21,36], we subjected them to MALDI-TOF analysis following deglycosylation. As expected, the purified proteins that were treated with glycopeptidase F yielded one major signal (rMCP-5: *m*/*z* 25 578, mMCP-5: 25 540), which is in good agreement with the theoretical value (rMCP-5: 25 569, mMCP-5: 25 524).

The recombinant proenzymes were processed to the mature forms by treatment with bovine cathepsin C. N-Terminal amino acid sequence analysis of each protein treated with cathepsin C yielded the expected sequence NH_2-Ile-Ile-Gly-Gly-Thr-Glu-Pro, from which two amino acids (Gly-Glu) upstream of the propeptide had been removed. Mass spectrometry analysis also showed a reduction in molecular mass (about 200 mass units), corresponding to the propeptide Gly-Glu. Furthermore, the purified mature enzymes had slightly higher mobility than the proenzyme forms in the SDS/PAGE analysis (Fig. 1, lanes 2 and 4). These results indicate the appropriate processing of the proenzymes by cathepsin C.

The enzymatic activity of mature MCP-5s and the V216G mutant of mMCP-5 was titrated with α1-antitrypsin and α1-antichymotrypsin, respectively. The activity of the recombinant proteases was inhibited at a molar ratio of inhibitor/protease of 1 : 1, indicating that the purified enzymes were enzymatically active (Fig. 2).

Analysis of substrate specificity

Because of the high amino acid sequence homology with other α-chymases, such as human and dog chymases, we assumed that both mMCP-5 and rMCP-5 were neutral serine proteases with chymotrypsin-like activity. However, when we exposed them to a typical chymase substrate, succinyl-Ala-His-Pro-Phe-*p*NA under neutral conditions, neither enzyme exhibited catalytic activity against it. We therefore screened MCP-5s against a large set of synthetic peptidyl substrates to ascertain whether the proteins possessed enzymatic activity. As shown in Table 1, under neutral (pH 8.5) and high-ionic strength (3 M NaCl) conditions, the recombinant MCP-5s clearly hydrolyzed elastase substrates that contained small or medium aliphatic amino acids (Ala, Ile, Val) in the P1 site, but they displayed no chymase, trypsin, or other kinds of protease activity. The enzymes showed a preference for the P1 site of the following substrates in the order: Val > Ile > Ala. They are also likely to prefer the proline residue in the P2 site of substrates, as observed in human chymase [37,38]. They hydrolyzed the methylated substrate MeO-succinyl-Ala-Ala-Pro-Val-*p*NA more effectively than the unmethylated succinyl-Al-Ala-Pro-Val-*p*NA, predominantly due to the lower K_m values. The enzyme activities of MCP-5s against peptidyl chromogenic substrates were relatively low compared with human chymase. Despite having a K_m value roughly similar to that of human chymase, the k_{cat} values were 70–80 times lower when tested by using each one's optimum substrate.

Site-directed mutagenesis

The three amino acid residues at positions 189, 216, and 226 (according to chymotrypsinogen numbering), comprising the substrate binding site, are generally responsible for controlling the primary substrate specificity of serine proteases [39]. For example, in chymotrypsin-like proteases, such as bovine chymotrypsin A, they are Ser189, Gly216, and Gly226, and consist of a broad primary specificity (S1) pocket that allows an aromatic sidechain of the substrate to penetrate into the pocket. By contrast, in elastases, such as human neutrophil elastase (HNE) and porcine pancreatic elastase (PPE), the 216th amino acid, which is located at the rim of the S1 pocket, is a valine that fills up most of the pocket with its hydrophobic sidechain. As a result, only substrates that have amino acids with small or medium sidechains in the P1 site, such as alanine and valine, can bind the S1 pocket [39,40]. Based on this knowledge, we carried out a multiple alignment of α- and β-chymases and, as expected, found that both MCP-5s possessed a Val216, as does HNE (Fig. 3).

In order to define the determinant residues for the substrate specificity of MCP-5, we prepared recombinant mMCP-5 mutant possessing a Gly substitution of Val at position 216 (V216G). Although slight elastase-like activity

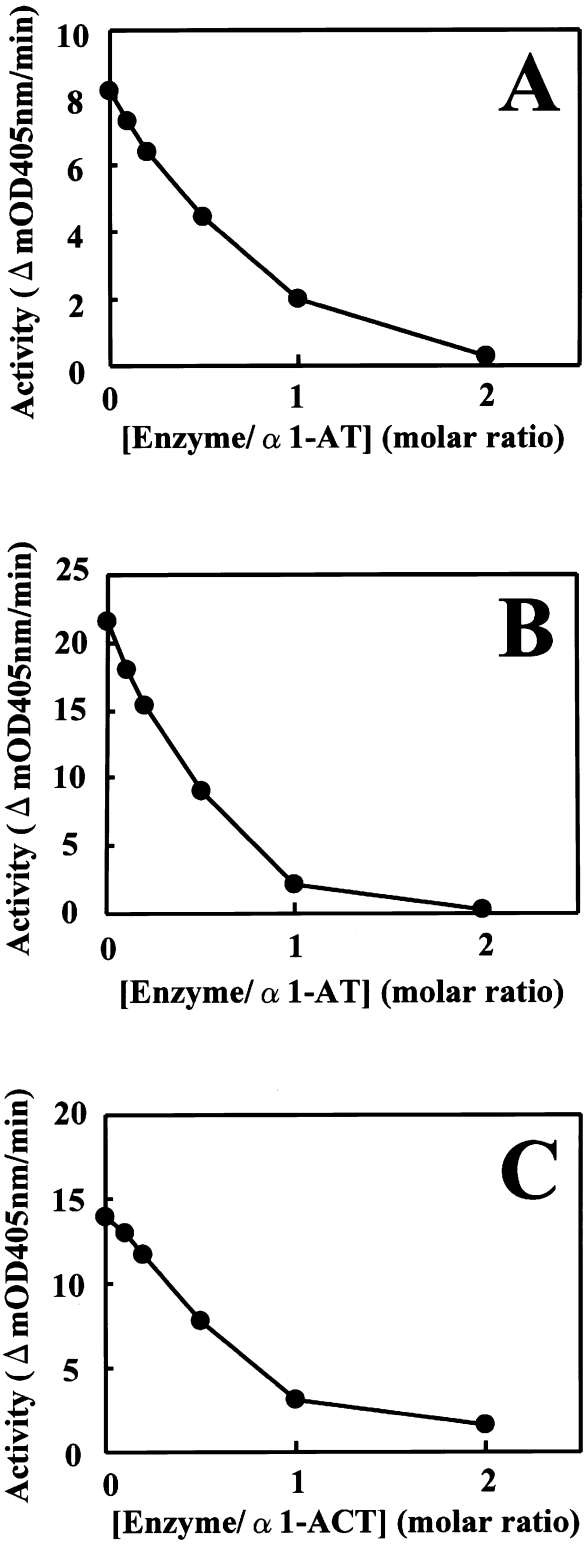

Fig. 2. Active site titration of MCP-5s with protease inhibitors. Each protease inhibitor was added to samples of (A) rMCP-5 (B) mMCP-5, and (C) the V216G mutant of mMCP-5 at the various molar ratios indicated. After 18 h incubation at 4 °C, residual activitiy was measured with the chromogenic peptidyl substrates used in inhibitor profiling.

remained, the mutant clearly exhibited activity against chymase substrate succinyl-Ala-His-Pro-Phe-*p*NA and succinyl-Ala-Ala-Phe-*p*NA, as expected (Table 1), indicating that the Val216 of mMCP-5 is a determinant residue of the substrate specificity.

Inhibitor profiles

Synthetic and natural protease inhibitors were used to test the enzymatic properties of recombinant MCP-5s, and human chymase and HNE were used as controls. Table 2 summarizes the effects of inhibitors on enzyme activities. Phenylmethylsulfonyl fluoride, which is the typical synthetic serine protease inhibitor, caused clear inhibition. Among the protein inhibitors, the serum elastase inhibitors SLPI, α1-AT, and Knitz-type inhibitor SBTI, produced clear inhibition (100% inhibition at 10 $\mu g \cdot mL^{-1}$, 20–50% inhibition at 10 $\mu g \cdot mL^{-1}$, and 40–60% inhibition at 10 $\mu g \cdot mL^{-1}$, respectively). α1-ACT and chymostatin, which are specific for chymotrypsin-like proteases, also inhibited the activity of MCP-5s (50–90% inhibition at 10 $\mu g \cdot mL^{-1}$ and 50–90% at 100 μM, respectively). The V216G mutant of mMCP-5 was more sensitive to chymostatin and α1-AT than the wild type (99% inhibition at 5 μM and 64% at 100 μM, respectively). Other protease inhibitors, aprotinin, leupeptin, pepstatin A, EDTA, bestatin, and E-64, had little or no effect on their activity (data not shown). These results indicated that the MCP-5s are serine proteases that are sensitive to inhibitors of chymotrypsin-like protease.

Elastolytic activity

As expected based on their substrate specificity, MCP-5s exhibited elastolytic activity. The amounts of DQ®-elastin degraded by each enzyme were linearly related to the enzyme concentration (Fig. 4A), but their activity was relatively low compared with that of HNE (Fig. 4B). When compared using parallel assays, the specific activities were approximately 100–200th that of HNE.

DISCUSSION

A striking finding in the present study is that based on their substrate specificity and inhibitor profiles, rodent α-chymases are elastase-like serine proteases. To our knowledge, the mast cell chymases that have been enzymatically characterized to date are all chymotrypsin-like proteases, without exception. Thus, this is the first report of chymases with elastase-like activity.

An enzyme assay using peptidyl chromogenic substrates clearly showed that both MCP-5s were elastase-like proteases that are most active against substrates with a valine in the P1 site and that their specificities are quite similar to that of HNE [41]. This strongly suggests a structural similarity of the substrate-binding sites of MCP-5s and HNE. The detailed structure of HNE has been investigated by X-ray crystallography [42], and examination of the complex between HNE and the third domain of turkey ovomucoid, a protein protease inhibitor, has shown that the S1 pocket can accommodate the small aliphatic amino acids Val, Ala, and Leu and is constricted toward its bottom by residues Val190, Phe192, Ala213, Val216, and Phe228. The corresponding residues in MCP-5s are exactly same as those of

Table 1. Kinetic constants for the hydrolysis of chromogenic peptidyl substrates of MCP-5s and human chymase. The reactions were initiated with enzymes, and change in absorbance at 405 nm was monitored continuously at 25 °C for 5 min. Assays were performed in triplicate, and the values are averages of two or three determinations. ND, not detected; NT, not tested.

Enzyme	Substrate	K_m (mM)	k_{cat} (s^{-1})	k_{cat}/K_m ($mM^{-1}·s^{-1}$)
rMCP-5	MeO-suc-AAPV-*p*NA	0.95	0.72	0.76
	Suc-AAPV-*p*NA	1.7	0.52	0.30
	Suc-AAPI-*p*NA	0.97	0.12	0.13
	Suc-APA-*p*NA	2.9	0.19	0.065
	Suc-AAV-*p*NA	3.2	0.059	0.019
	Suc-AHPF-*p*NA			ND
	Suc-AAF-*p*NA			ND
mMCP-5	MeO-suc-AAPV-*p*NA	0.29	0.75	2.6
	Suc-AAPV-*p*NA	0.78	0.91	1.2
	Suc-AAPI-*p*NA	0.39	0.15	0.37
	Suc-APA-*p*NA	2.6	0.20	0.076
	Suc-AAV-*p*NA	2.8	0.049	0.018
	Suc-AHPF-*p*NA			ND
	Suc-AAF-*p*NA			ND
mMCP-5 V216G	MeO-suc-AAPV-*p*NA	0.88	0.30	0.34
	Suc -AAPV-*p*NA	1.6	0.29	0.18
	Suc-AAPI-*p*NA	0.87	0.082	0.093
	Suc-APA-*p*NA			NT
	Suc-AAV-*p*NA			NT
	Suc-AHPF-*p*NA	0.12	0.85	7.3
	Suc-AAF-*p*NA	0.33	0.18	0.56
Human chymase	MeO-suc-AAPV-*p*NA			ND
	Suc-AAPV-*p*NA			ND
	Suc-AAPI-*p*NA			ND
	Suc-APA-*p*NA			ND
	Suc-AAV-*p*NA			ND
	Suc-AHPF-*p*NA	0.12	62	510
	Suc-AAF-*p*NA	0.12	26	230

HNE, except Phe192, but they are different from those of HNE, except for Phe228, in the chymases of primates and dogs (Fig. 3). This demonstrates that the S1 pockets of MCP-5s are quite similar in size and shape to that of HNE.

Among the elastase substrates, MCP-5s displayed a preference for substrates with the proline residue in the P2 site, and this preference has also been observed in various serine proteases, such as HNE [41], human chymase [37,38], and thrombin [42]. According to X-ray crystallography of HNE and human chymase [43,44], the P2 proline-directed preference is due to the bowl-shaped and quite hydrophobic S2 pockets that consist of Leu99, Phe215 (Tyr215 in human chymase), and the flat side of the imidazole ring of His57. Thus, the preference of MCP-5s is probably due to the hydrophobic S2 pockets that consist of Val99, Tyr215, and His57, similar to HNE and human chymase.

Based on the profiles of the protease inhibitors, MCP-5s were concluded to be serine proteases the same as other chymases. The serum protease inhibitors SLPI and α1-AT, which are known to be predominant inhibitors of serine proteases, such as HNE, cathepsin G, and chymases [45,46], effectively inhibited MCP-5s. As these inhibitors are thought to play a role in protecting tissues from injury associated with inflammation caused by proteases, our results suggest that MCP-5s are also inflammatory mediators released from mast cells and the physiological targets of these inhibitors. Unexpectedly, the MCP-5s were sensitive to chymostatin and α1-ACT, which are specific for chymotrypsin-like proteases, in despite of their elastase-like specificity. This may be due to the subtle difference in binding site between elastase substrates and inhibitors. Further studies, such as inhibition kinetic analysis and detailed structural analysis for MCP-5-chymostatin complex by X-ray crystallography, are necessary to clarify the mechanism of the inhibition.

Site-directed mutagenesis analysis for mMCP-5 showed that Val216 is a determinant residue for the elastase-like specificity. The V216G mutant exhibited activity against chymase substrates with Phe in their P1 sites and displayed higher sensitivity to chymostatin and α1-ACT than the wild type (Tables 1 and 2), suggesting that the mutant has enzyme specificity similar to that of human chymase. More recently, Solivan *et al.* [47] have reported conversion of human chymase into an elastase-like protease by a G216V mutation. Although they suggested the elastase-like specificity of chymase with Val216, our findings have directly demonstrated the validity of their prediction.

The homology models of the mMCP-5 and the V216G mutant were consistent with the results of the enzyme assays. Similar to HNE [42], Val216 was located at the rim

```
                                                *
Bovine Chymotrypsinogen     188 VSSCMGDSGGPLVCKKNGAWTLVGIVSWGSSTCSTST-PGVYAR 230
Human Chymase                   KSAFKGDSGGPLLCAG----VAQGIVSYGRSDAKP---PAVFTR
Baboon Chymase                  KSAFKGDSGGPLLCAG----VAQGIVSYGRLDAKP---PAVFTR
Crab-eating macaque Chymase     KSAFKGDSGGPLLCAG----VAQGIVSYGRLDAKP---PAVFTR
Dog Chymase                     KSAFKGDSGGPLLCAG----VAQGIVSYGQNDAKP---PAVFTR
Sheep MCP-2                     KSAFKGDSGGPLLCAG----VAQGIVSYGLSSAKP---PAVFTR
mMCP-1                          KTAYMGDSGGPLLCAG----VAHGIVSYGDSHGKP---PAVFTR
mMCP-4                          RSAYKGDSGGPLLCAG----VAHGIVSYGRGDAKP---PAVFTR
mMCP-9                          ASVYMGDSGGPLLCAG----VAHGIVSSGRGNAKP---PAIFTR
rMCP-1                          RSAYKGDSGGPLVCAG----VAHGIVSYGRGDAKP---PAVFTR
rMCP-2                          RAAFMGDSGGPLLCAG----VAHGIVSYGHPDAKP---PAIFTR
Rat Vascular Chymase            QTAYTGDSGGPLLCAG----VVHGIVSYGHPDATP---PAVFTR
Mongolian gerbil MCP-1          RSAYKGDSGGPLVCAG----VAHGIVSYGRIDAKP---PAVFTR
Hamster Chymase-1               RSAYKGDSGGPLLCAG----VAHGIVSYGRGDAKP---PAVFTR

Human Neutrophil Elastase       AGVCFGDSGSPLVCNG----LIHGIASFVRGGCASGLYPDAFAP
mMCP-5                          QNVYKGDSGGPLLCAG----IAQGIASYVHRNAKP---PAVFTR
rMCP-5                          QNVYKGDSGGPLLCAG----IAQGIASYVHPNAKP---PAVFTR
Mongolian gerbil MCP-2          QNVYKGDSGGPLLCAG----IAQGIASYVRRNARP---PAVFTR
Hamster Chymase-2               RNVYKGDSGGPLLCAG----IAQGIASYVLRNAKP---PSVFTR
```

Fig. 3. Multiple alignments of amino acid sequences of chymases. Amino acid sequences of chymases, human neutrophil elastase, and bovine chymotrypsinogen A were aligned using the CLUSTAL W program [35]. The figure shows part of the aligned sequences (amino acids at 188–230 in chymotrypsinogen numbering). Amino acids at position 216 are marked by an asterisk. The hyphens in each line indicate alignment gaps. The amino acid sequences of the proteases were obtained from the NCBI protein database (bovine chymotrypsinogen A: KYBOA, human neutrophil elastase: P08246, human chymase: P23946, baboon chymase: P52195, crab-eating macaque chymase: P56435, dog chymase: A35842, sheep MCP-2: P79204, mMCP-1: AAB23194, mMCP-2: NP_032597, mMCP-4: A46721, mMCP-5: P21844, mMCP-9: O35164, rMCP-1: P09650, rMCP-2: P00770, rMCP-4: P97592, rMCP-5: NP_037224, mongolian gerbil MCP-1: g2137100, mongolian gerbil MCP-2: g4502907, hamster chymase-1: BAA19932, hamster chymase-2: BAA28615).

of the S1 pocket, which was partially occluded by the sidechain of Val216 (Fig. 5, lower panel, left). By contrast, the S1 pocket of the V216G mutant was relatively broad compared with the wild type (Fig. 5, lower panel, right) and seemed to be adequate for penetration by the aromatic amino acid in the P1 site of the substrate.

Rodent mast cells are generally classified into two subsets based on differences in the proteoglycans and serine proteases present in their granules: connective tissue mast cells (CTMCs) and mucosal mast cells (MMCs). CTMCs are widely distributed in connective tissue of whole body, such as in the skin, airway submucosa, and cardiovascular tissues. They are regarded as critical effector cells in the allergic inflammatory reaction to exclude antigens by releasing various inflammatory mediators, and they contribute to the development and modulation of other inflammatory and physiological processes, such as tissue fibrosis [48] and angiogenesis [49]. As MCP-5s are predominantly expressed in CTMCs along with α-chymases (mMCP-4, rMCP-1) *in vivo* [35,50], it is likely that MCP-5s are involved in the biological functions of CTMCs. Here, we have shown that MCP-5s have obvious elastolytic activity, and this suggests that they act as elastolytic proteases under physiological conditions and are involved in elastolysis by CTMCs. However, little is known about the relationships between mast cells and elastolysis. In animal studies using rats, Tozzi *et al.* [51,52] recently showed that the regression of remodeling in the pulmonary arteries induced by normoxia following exposure of hypoxia was accompanied by elastolytic activity of serine protease and CTMC accumulation in the outer walls of pulmonary arteries. Although such serine proteases have not fully been characterized, their activity may be derived from rMCP-5 expressed by CTMCs. On the other hand, the elastolytic activity of MCP-5s was much lower than that of HNE (Fig. 4), suggesting that there are some differences in the function of the elastolytic enzyme between MCP-5s and HNE *in vivo*. Further animal studies using mice and rats may be necessary to clarify this.

The α-chymases of primates and dogs have highly specific activity converting angiotensin (Ang) I into Ang II [22,28,53], and based on the results of animal studies, they are believed to contribute to the pathogenesis of cardiovascular diseases such as cardiomyopathy [54], myocardial infarction [55], atherosclerosis [22], and balloon injury induced intimal hyperplasia [56,57] via Ang II generation.

Table 2. Effect of protease inhibitors on the enzyme activity of MCP-5s, human chymase and HNE. Enzymes were preincubated with the inhibitors on ice for 10 min, and the reaction was initiated with each substrate solution. Residual activity was monitored, and percent inhibition was calculated from the uninhibited rate. Assays were performed in triplicate, and the values are averages of two or three determinations. NT, not tested; NI, no inhibition.

		% Inhibition				
Inhibitor	Concentration	rMCP-5	mMCP-5	mMCP-5 V216G	Human chymase	HNE
Phenylmethylsulfonyl fluoride	1 mM	100	100	NT[a]	100	100
SLPI	1 μg·mL^{-1}	41	66	71	93	99
	10 μg·mL^{-1}	100	100	100	97	100
SBTI	10 μg·mL^{-1}	59	39	62	95	81
	100 μg·mL^{-1}	100	92	99	99	97
α_1-AT	10 μg·mL^{-1}	49	22	15	22	99
	100 μg·mL^{-1}	100	100	64	79	100
α_1-ACT	10 μg·mL^{-1}	51	92	83	100	5
	100 μg·mL^{-1}	98	97	NT	NT	22
Chymostatin	20 μM	15	30	100	99	NI
	100 μM	48	87	100	100	NI

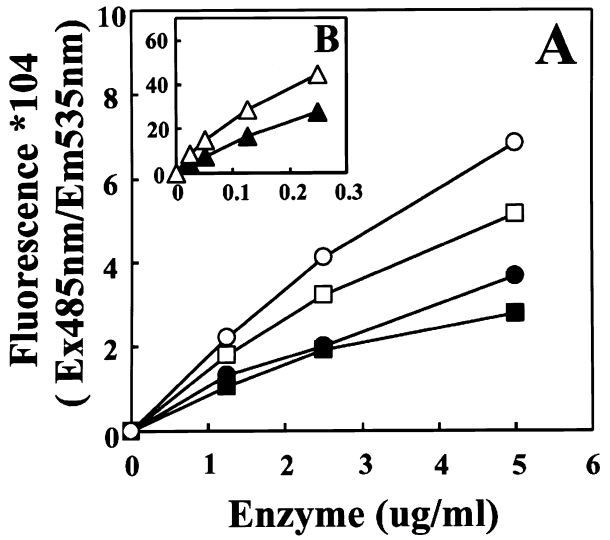

Fig. 4. Elastolytic activity of MCP-5s. Aliquots of DQ^{TM} elastin at a final concentration of 25 μg·mL^{-1} were incubated with various concentrations of MCP-5s (A) and HNE (B) in a 96-well microplate. After incubation times of 60 and 150 min, fluorescence was measured at an excitation wavelength of 485 nm and an emission wavelength of 535 nm with a Wallac 1420 ARVO-sx Multi-label counter. ○, rMCP-5 (150 min); □, mMCP-5 (150 min); △, HNE (150 min); ●, rMCP-5 (60 min); ■, mMCP-5 (60 min); ▲, HNE (60 min). Assays were performed in triplicate.

Rodent β-chymases, on the other hand, degrade Ang I by cleaving the peptide bond of Tyr4 and Ile-5 [18,58]. Consequently, Ang II formation in cardiovascular tissues

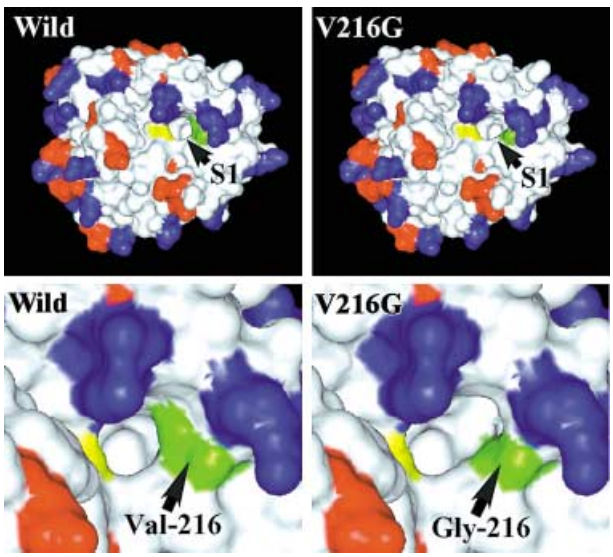

Fig. 5. S1 pocket structures of mMCP-5 and the V216G mutant. Homology models of the mMCP-5 and V216G mutant were produced using MODELLER as described in Experimental procedures. Upper panels, left and right: surface representation of the whole molecules of the mMCP-5 and the V216G mutant, respectively. The S1 binding pockets are shown. Lower panels, left and right: the enlarged views are from the perspective of the S1 pocket. Green indicates the amino acid at position 216 located in the rim of the S1 pocket. Yellow indicates catalytic center Ser195. Blue and red indicate basic and acidic residues, respectively, and all other residues are colored gray.

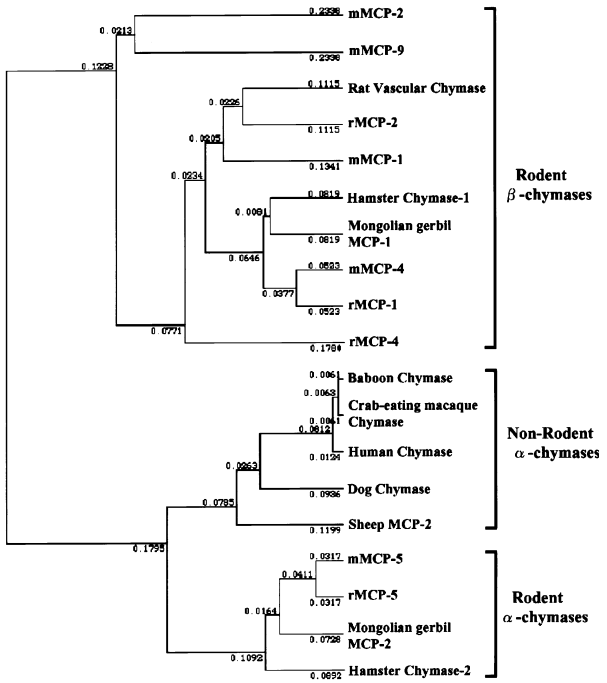

Fig. 6. Phylogenetic relations based on alignment of α- and β-chymases. The phylogenetic tree was derived by the UPGMA method performed by the GENETYX-MAC program (Software Corp., Tokyo, Japan). The sequence divergence between any pair of sequences is equal to the sum of the length of the horizontal branches connecting the two sequences.

is almost completely ACE-dependent in rodents, whereas it is mainly chymase-dependent in primates and dogs [59,60]. In our experiments, MCP-5s exhibited no catalytic activitiy against Ang I (data not shown). This is a clear example of a difference in specificity to natural substrates between rodent and nonrodent α-chymases. Similar to β-chymases, MCP-5s may be key enzymes responsible for the species difference in the local Ang-II forming system.

The species difference in substrate specificity between rodent and nonrodent α-chymases is a matter of interest from the standpoint of molecular evolution. Multiple alignments of α- and β-chymases have revealed that the rodent chymases hamster chymase-2 and mongolian gerbil MCP-2 contain Val216 the same as MCP-5s (Fig. 3) and have high sequence homology with MCP-5s (more than 80%). Furthermore, a phylogenetic tree based on multiple alignments has revealed that the chymase family can be divided into three groups: rodent β-chymases with Gly216, nonrodent α-chymases with Gly216, and rodent α-chymases with Val216 (Fig. 6). These results strongly suggest that all four rodent α-chymases are elastase-like proteases that are evolutionarily close to each other.

The chymase phylogenetic tree provides information on the period when the substrate specificity conversion into elastase-like protease occurred during molecular evolution. Chandrasekharan *et al.* [18] reconstructed 'ancestral chymase' by means of phylogenetic inferences and showed that it possessed Gly216 and highly specific Ang II forming (chymotrypsin-like) activity. Given their inferences and the branching order of our phylogenetic tree, the conversion into elastase must have occurred after branching into rodent

and nonrodent chymases (a common ancestor of primates, dogs, and sheep) in the evolutionary process. Although less is known about what the specificity of the conversion means, further studies by analysis of natural substrates and genetically engineered mice, such as mMCP-5 gene knock-out or knock-in mice, will help to elucidate its function *in vivo*.

Our present study clearly showed that rodent α-chymases are elastase-like proteases having elastolytic activity, and thus it may be more appropriate to refer to them as 'mast cell elastases'. Although their functions are not fully defined here, their substrate specificities suggest that they possess unique physiological roles different from those of chymases with chymotrypsin-like activity.

ACKNOWLEDGMENTS

We thank Dr Satoshi Yamamura for technical advice in preparing the recombinant proteins.

REFERENCES

1. Walls, A.F. (1998) *Mast Cell Proteases in Asthma, Inflammatory Mechanisms in Asthma* (Holgate, S., T., Busse, W. & W., eds), pp. 89–110. Marcel Dekker, New York.
2. Caughey, G.H. (1995) *Mast Cell Proteases in Immunology and Biology*. Marcel Dekker, Basel.
3. He, S. & Walls, A.F. (1998) Human mast cell chymase induces the accumulation of neutrophils, eosinophils and other inflammatory cells *in vivo*. *Br. J. Pharmacol.* **125**, 1491–1500.
4. He, S. & Walls, A.F. (1998) The induction of a prolonged increase in microvascular permeability by human mast cell chymase. *Eur. J. Pharmacol.* **352**, 91–98.
5. Tani, K., Ogushi, F., Kido, H., Kawano, T., Kunori, Y., Kamimura, T., Cui, P. & Sone, S. (2000) Chymase is a potent chemoattractant for human monocytes and neutrophils. *J. Leukoc. Biol.* **67**, 585–589.
6. Sommerhoff, C.P., Caughey, G.H., Finkbeiner, W.E., Lazarus, S.C., Basbaum, C.B. & Nadel, J.A. (1989) Mast cell chymase. A potent secretagogue for airway gland serous cells. *J. Immunol.* **142**, 2450–2456.
7. Katunuma, N., Fukusen, N. & Kido, H. (1986) Biological functions of serine proteases in the granules of rat mast cells. *Adv. Enzyme Regul.* **25**, 241–255.
8. Vartio, T., Seppa, H. & Vaheri, A. (1981) Susceptibility of soluble and matrix fibronectins to degradation by tissue proteinases, mast cell chymase and cathepsin G. *J. Biol. Chem.* **256**, 471–477.
9. Kofford, M.W., Schwartz, L.B., Schechter, N.M., Yager, D.R., Diegelmann, R.F. & Graham, M.F. (1997) Cleavage of type I procollagen by human mast cell chymase initiates collagen fibril formation and generates a unique carboxyl-terminal propeptide. *J. Biol. Chem.* **272**, 7127–7131.
10. Mayer, U., Mann, K., Timpl, R. & Murphy, G. (1993) Sites of nidogen cleavage by proteases involved in tissue homeostasis and remodelling. *Eur. J. Biochem.* **217**, 877–884.
11. Gruber, B.L. & Schwartz, L.B. (1990) The mast cell as an effector of connective tissue degradation: a study of matrix susceptibility to human mast cells. *Biochem. Biophys. Res. Commun.* **171**, 1272–1278.
12. Banovac, K., Banovac, F., Yang, J. & Koren, E. (1993) Interaction of osteoblasts with extracellular matrix: effect of mast cell chymase. *Proc. Soc. Exp. Biol. Medical* **203**, 221–235.
13. Banovac, K. & De Forteza, R. (1992) The effect of mast cell chymase on extracellular matrix: studies in autoimmune thyroiditis and in cultured thyroid cells. *Int. Arch. Allergy Immunol.* **99**, 141–149.
14. Taipale, J., Lohi, J., Saarinen, J., Kovanen, P.T. & Keski-Oja, J. (1995) Human mast cell chymase and leukocyte elastase release latent transforming growthfactor-beta 1 from the extracellular matrix of cultured human epithelial and endothelial cells. *J. Biol. Chem.* **270**, 4689–4696.
15. Longley, B.J., Tyrrell, L., Ma, Y., Williams, D.A., Halaban, R., Langley, K., Lu, H.S. & Schechter, N.M. (1997) Chymase cleavage of stem cell factor yields a bioactive, soluble product. *Proc. Natl Acad. Sci. U.S.A* **94**, 9017–9021.
16. Mizutani, H., Schechter, N., Lazarus, G., Black, R.A. & Kupper, T.S. (1991) Rapid and specific conversion of precursor interleukin 1 beta (IL-1 beta) to an active IL-1 species by human mast cell chymase. *J. Exp. Med.* **174**, 821–825.
17. Tunon de Lara, J.M., Okayama, Y., McEuen, A.R., Heusser, C.H., Church, M.K. & Walls, A.F. (1994) Release and inactivation of interleukin-4 by mast cells. *Ann. NY Acad. Sci.* **725**, 50–58.
18. Chandrasekharan, U.M., Sanker, S., Glynias, M.J., Karnik, S.S. & Husain, A. (1996) Angiotensin II-forming activity in a reconstructed ancestral chymase. *Science* **271**, 502–505.
19. Huang, R. & Hellman, L. (1994) Genes for mast-cell serine protease and their molecular evolution. *Immunogenetics* **40**, 397–414.
20. Reynolds, D.S., Stevens, R.L., Lane, W.S., Carr, M.H., Austen, K.F. & Serafin, W.E. (1990) Different mouse mast cell populations express various combinations of at least six distinct mast cell serine proteases. *Proc. Natl Acad. Sci. U.S.A* **87**, 3230–3234.
21. Lutzelschwab, C., Pejler, G., Aveskogh, M. & Hellman, L. (1997) Secretory granule proteases in rat mast cells. Cloning of 10 different serine proteases and a carboxypeptidase A from various rat mast cell populations. *J. Exp. Med.* **185**, 13–29.
22. Takai, S., Shiota, N., Kobayashi, S., Matsumura, E. & Miyazaki, M. (1997) Induction of chymase that forms angiotensin II in the monkey atherosclerotic aorta. *FEBS Lett.* **412**, 86–90.
23. Caughey, G.H., Raymond, W.W. & Vanderslice, P. (1990) Dog mast cell chymase: molecular cloning and characterization. *Biochemistry* **29**, 5166–5171.
24. Caughey, G.H., Zerweck, E.H. & Vanderslice, P. (1991) Structure, chromosomal assignment, and deduced amino acid sequence of a human gene for mast cell chymase. *J. Biol. Chem.* **266**, 12956–12963.
25. Powers, J.C., Tanaka, T., Harper, J.W., Minematsu, Y., Barker, L., Lincoln, D., Crumley, K.V., Fraki, J.E., Schechter, N.M. & Lazarus, G.G. (1985) Mammalian chymotrypsin-like enzymes. Comparative reactivities of rat mast cell proteases, human and dog skin chymases, and human cathepsin G with peptide 4-nitroanilide substrates and with peptide chloromethyl ketone and sulfonyl fluoride inhibitors. *Biochemistry* **24**, 2048–2058.
26. Newlands, G.F., Knox, D.P., Pirie-Shepherd, S.R. & Miller, H.R. (1993) Biochemical and immunological characterization of multiple glycoforms of mouse mast cell protease 1: comparison with an isolated murine serosal mast cell protease (MMCP-4). *Biochem. J.* **294** (1), 127–135.
27. Reilly, C.F., Tewksbury, D.A., Schechter, N.M. & Travis, J. (1982) Rapid conversion of angiotensin I to angiotensin II by neutrophil and mast cell proteinases. *J. Biol. Chem.* **257**, 8619–8622.
28. Urata, H., Kinoshita, A., Misono, K.S., Bumpus, F.M. & Husain, A. (1990) Identification of a highly specific chymase as the major angiotensin II- forming enzyme in the human heart. *J. Biol. Chem.* **265**, 22348–22357.
29. Kido, H., Nakano, A., Okishima, N., Wakabayashi, H., Kishi, F., Nakaya, Y., Yoshizumi, M. & Tamaki, T. (1998) Human chymase, an enzyme forming novel bioactive 31-amino acid length endothelins. *Biol. Chem.* **379**, 885–891.
30. Shiota, N., Saegusa, Y., Nishimura, K. & Miyazaki, M. (1997) Angiotensin II-generating system in dog and monkey ocular tissues. *Clin. Exp. Pharmacol. Physiol.* **24**, 243–248.

31. Ho, S.N., Hunt, H.D., Horton, R.M., Pullen, J.K. & Pease, L.R. (1989) Site-directed mutagenesis by overlap extension using the polymerase chain reaction. *Gene* **77**, 51–59.
32. Bairoch, A. & Boeckmann, B. (1991) The SWISS-PROT protein sequence data bank. *Nucl Acids Res.* **19** (Suppl.), 2247–2249.
33. Sali, A. & Blundell, T.L. (1993) Comparative protein modelling by satisfaction of spatial restraints. *J. Mol. Biol.* **234**, 779–815.
34. Laemmli, U. K. (1970) Cleavage of structural proteins during the assembly of the head of bacteriophage T4. *Nature* **227**, 680–685.
35. Thompson, J.D., Higgins, D.G. & Gibson, T.J. (1994) CLUSTAL W: improving the sensitivity of progressive multiple sequence alignment through sequence weighting, position-specific gap penalties and weight matrix choice. *Nucl Acids Res.* **22**, 4673–4680.
36. McNeil, H.P., Austen, K.F., Somerville, L.L., Gurish, M.F. & Stevens, R.L. (1991) Molecular cloning of the mouse mast cell protease-5 gene. A novel secretory granule protease expressed early in the differentiation of serosal mast cells. *J. Biol. Chem.* **266**, 20316–20322.
37. Caughey, G.H., Raymond, W.W. & Wolters, P.J. (2000) Angiotensin II generation by mast cell a. *Biochim. Biophys. Acta* **1480**, 245–257.
38. Kinoshita, A., Urata, H., Bumpus, F.M. & Husain, A. (1991) Multiple determinants for the high substrate specificity of an angiotensin II-forming chymase from the human heart. *J. Biol. Chem.* **266**, 19192–19197.
39. Kraut, J. (1977) Serine proteases: structure and mechanism of catalysis. *Annu. Rev. Biochem.* **46**, 331–358.
40. Shotton, D.M. & Watson, H.C. (1970) The three-dimensional structure of crystalline porcine pancreatic elastase. *Philos. Trans. R. Soc. Lond. B Biol. Sci.* **257**, 111–118.
41. Nakajima, K., Powers, J.C., Ashe, B.M. & Zimmerman, M. (1979) Mapping the extended substrate binding site of cathepsin G and human leukocyte elastase. Studies with peptide substrates related to the alpha 1-protease inhibitor reactive site. *J. Biol. Chem.* **254**, 4027–4032.
42. McRae, B.J., Kurachi, K., Heimark, R.L., Fujikawa, K., Davie, E.W. & Powers, J.C. (1981) Mapping the active sites of bovine thrombin, factor IXa, factor Xa, factor XIa, factor XIIa, plasma kallikrein, and trypsin with amino acid and peptide thioesters: development of new sensitive substrates. *Biochemistry* **20**, 7196–7206.
43. Bode, W., Meyer, E. Jr & Powers, J.C. (1989) Human leukocyte and porcine pancreatic elastase: X-ray crystal structures, mechanism, substrate specificity, and mechanism-based inhibitors. *Biochemistry* **28**, 1951–1963.
44. Pereira, P.J., Wang, Z.M., Rubin, H., Huber, R., Bode, W., Schechter, N.M. & Strobl, S. (1999) The 2.2 A Crystal Structure of Human Chymase in Complex with Succinyl- Ala-Ala-Pro-Phe-chloromethylketone: Structural Explanation for its Dipeptidyl Carboxypeptidase Specificity. *J. Mol. Biol.* **286**, 817.
45. Fritz, H. (1988) Human mucus proteinase inhibitor (human MPI). Human seminal inhibitor I (HUSI-I), antileukoprotease (ALP), secretory leukocyte protease inhibitor (SLPI). *Biol. Chem. Hoppe Seyler* **369** (Suppl.), 79–82.
46. Carrell, R.W. & Boswell, D.R. (1986) *Proteinase Inhibitors*. Elsevier Science, Publishers BV.
47. Solivan, S., Selwood, T., Wang, Z.M. & Schechter, N.M. (2002) Evidence for diversity of substrate specificity among members of the chymase family of serine proteases. *FEBS Lett.* **512**, 133–138.
48. Kaliner, M.A. & Metcalfe, D. (1993) *The Mast Cell in Health and Disease*. Marcel Dekker, Inc., New York.
49. Metcalfe, D.D., Baram, D. & Mekori, Y.A. (1997) Mast cells. *Physiol. Rev.* **77**, 1033–1079.
50. Ide, H., Itoh, H., Tomita, M., Murakumo, Y., Kobayashi, T., Maruyama, H., Osada, Y. & Nawa, Y. (1995) Cloning of the cDNA encoding a novel rat mast-cell proteinase, rMCP-3, and its expression in comparison with other rat mast-cell proteinases. *Biochem. J.* **311**, 675–680.
51. Tozzi, C.A., Thakker-Varia, S., Yu, S.Y., Bannett, R.F., Peng, B.W., Poiani, G.J., Wilson, F.J. & Riley, D.J. (1998) Mast cell collagenase correlates with regression of pulmonary vascular remodeling in the rat. *Am. J. Respir. Cell Mol. Biol.* **18**, 497–510.
52. Riley, D.J., Thakker-Varia, S., Wilson, F.J., Poiani, G.J. & Tozzi, C.A. (2000) Role of proteolysis and apoptosis in regression of pulmonary vascular remodeling. *Physiol. Res.* **49**, 577–585.
53. Shiota, N., Okunishi, H., Fukamizu, A., Sakonjo, H., Kikumori, M., Nishimura, T., Nakagawa, T., Murakami, K. & Miyazaki, M. (1993) Activation of two angiotensin-generating systems in the balloon-injured artery. *FEBS Lett.* **323**, 239–242.
54. Shiota, N., Fukamizu, A., Takai, S., Okunishi, H., Murakami, K. & Miyazaki, M. (1997) Activation of angiotensin II-forming chymase in the cardiomyopathic hamster heart. *J. Hypertens.* **15**, 431–440.
55. Jin, D., Takai, S., Yamada, M., Sakaguchi, M., Yao, Y. & Miyazaki, M. (2001) Possible roles of cardiac chymase after myocardial infarction in hamster hearts. *Jpn. J. Pharmacol.* **86**, 203–214.
56. Miyazaki, M., Wada, T., Shiota, N. & Takai, S. (1999) Effect of an angiotensin II receptor antagonist, candesartan cilexetil, on canine intima hyperplasia after balloon injury. *J. Hum. Hypertens.* **13** (Suppl. 1), S21–S25.
57. Shiota, N., Okunishi, H., Takai, S., Mikoshiba, I., Sakonjo, H., Shibata, N. & Miyazaki, M. (1999) Tranilast suppresses vascular chymase expression and neointima formation in balloon-injured dog carotid artery. *Circulation* **99**, 1084–1090.
58. Le Trong, H., Neurath, H. & Woodbury, R.G. (1987) Substrate specificity of the chymotrypsin-like protease in secretory granules isolated from rat mast cells. *Proc. Natl Acad. Sci. U.S.A* **84**, 364–367.
59. Jin, D., Takai, S., Yamada, M., Sakaguchi, M. & Miyazaki, M. (2000) The functional ratio of chymase and angiotensin converting enzyme in angiotensin I-induced vascular contraction in monkeys, dogs and rats. *Jpn. J. Pharmacol.* **84**, 449–454.
60. Balcells, E., Meng, Q.C., Johnson, W.H. Jr, Oparil, S. & Dell'Italia, L.J. (1997) Angiotensin II formation from ACE and chymase in human and animal hearts: methods and species considerations. *Am. J. Physiol.* **273**, H1769–H1774.